RV-W 우주비행기 열공력모우멘트 해석기법 최신 동향

July 6th (Thursday), 2023

명노신 (Rho-Shin Myong)

Professor, School of Aerospace and Software Engineering
Director, Research Center for Aircraft Core Technology (ERC)
Aerospace Computational Modeling Laboratory (ACML)
경상국립대학교 (Gyeongsang National University)
http://acml.gnu.ac.kr/
myong@gnu.ac.kr

Seminar at the Korea Aerospace Research Institute (KARI)

GNU 경상국립대학교 Gyeongsang National University

ASRC Aerospace Systems Research Center 항공우주시스템연구소

A brief history: Superaerodynamics

Albert F. Zahm (US)

"**Superaerodynamics**," Journal of the Franklin Institute, Vol. 217, pp. 153-166, **1934**.

Eugene Sänger (Austria)

Silbervogel ("Silverbird") (**1944**)

Ludwig Prandtl (Germany)

Theodore von Kármán (US, **1946**)

Hsue-shen Tsien (錢學森, US)

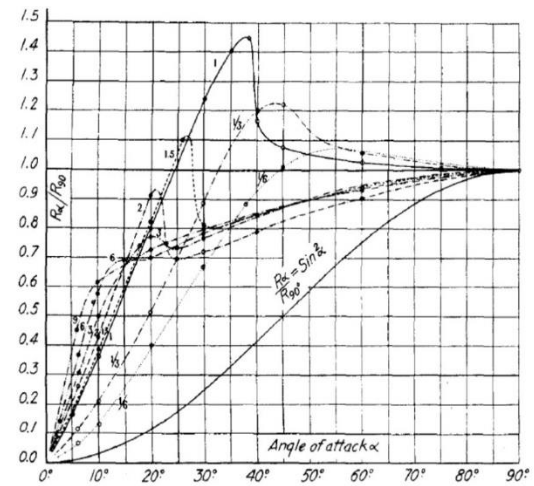

Values of ratio R_α/R_{90} for inclined rectangles of different aspect ratios, as found by Eiffel and by discrete-fluid formula $R_\alpha/R_{90} = \sin^2\alpha$.

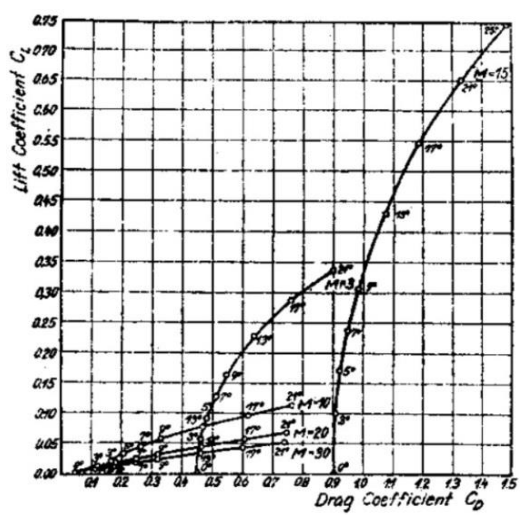

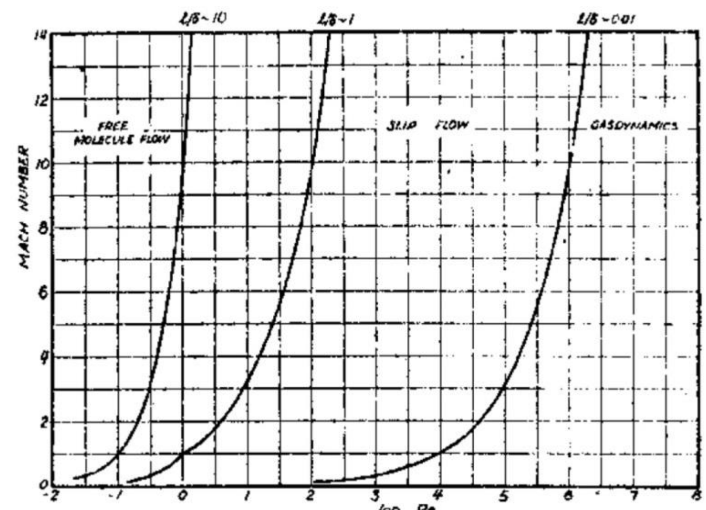

Munk (developer of the thin-airfoil theory) at NACA disliked Zahm's manuscript submitted to J. of the Aeronautical Sciences?

Recent trend in hypersonics

CAS JF-12 (2012; Mach 5-9,
Altitude 25-50km, 130 msec)

HGV (Hypersonic
Glider Vehicle)

CAS JF-22 (30 May 2023; 10 km/sec)

“China’s JF-22 hypersonic wind tunnel blows by US”
JF-22 detonation-driven high-enthalpy shock tunnel
“The goal of the JF-22 wind tunnel is to accelerate the development of a space-to-earth shuttle system.”(Zonglin Jiang) (ASIA Times on June 7, 2023)

Recent trend in reusable space plane

China's reusable Shenlong space plane

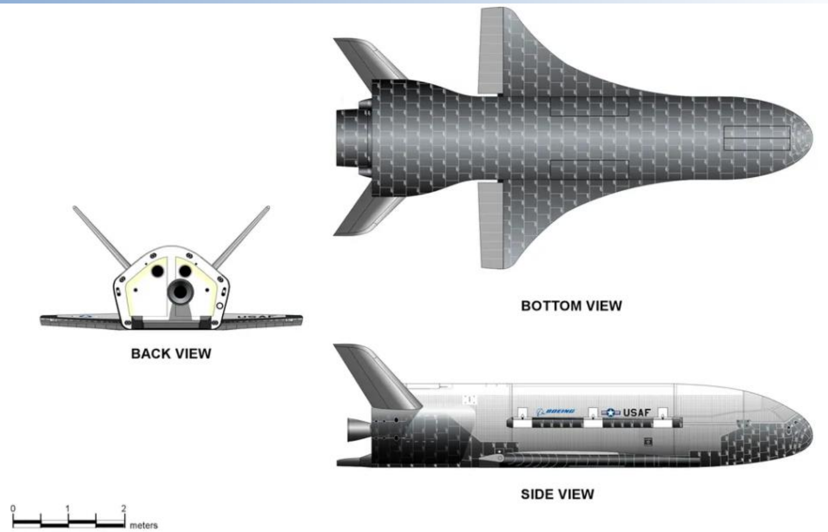

U.S. Space Force's robotic X-37B (Orbital Test Vehicle, OTV)

China's (robotic) space plane returns to Earth after 9-month orbital mission
Touched down Monday (May 8, 2023) at the Jiuquan Satellite Launch Center
(www.space.com on May 09, 2023)

6회 OTV-6/USSF 7(2호기) : 2020년 5월 17일 ~ 2022년 11월 12일, 총 980일 20시간
X-37B 4,990kg, 8.9 meters long, 4.5 wingspan
Atlas V 8,250 ~ 20,520kg (LEO), 4,750 ~ 8,900kg (GTO)
Falcon 9 22,800kg (LEO), 8,300kg (GTO)

낙하산으로 바다에 착수하는 오리온 다목적 유인 우주선(개발중)과 대비

참고: 누리호 3,300kg (LEO)
차세대 발사체 10,000kg (LEO)
(KSLV-III 개발 사업 2023-2032년 2조 132억원)

Winged Reentry Vehicles

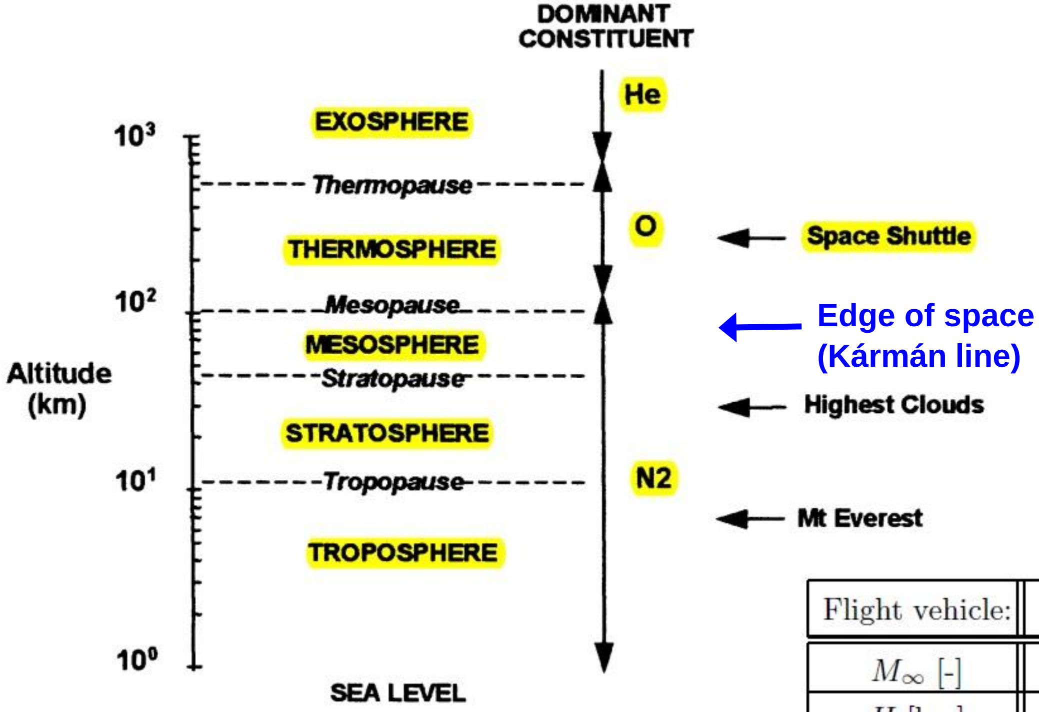

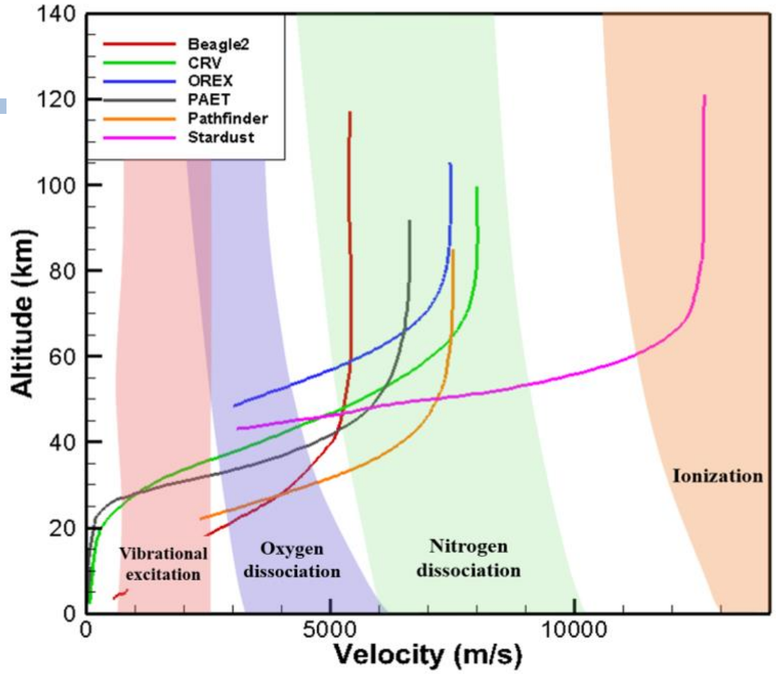

Flight vehicle:	RV-W 1	RV-W 2	CAV 1	CAV 2
M_∞ [-]	20	6	6.8	12
H [km]	70.0	40.0	30.0	34.2
α [°]	40.0	25.0	5.0	5.0
L_{ref} [m]	32.0	32.0	82.0	20.0
T_∞ [K]	219.69	250.33	226.51	234.27
v_∞ [m/s]	5,942.7	1,903.1	2,051.6	3,682.0
ρ_∞ [kg/m^3]	$8.75\cdot10^{-5}$	$4.0\cdot10^{-3}$	$1.84\cdot10^{-2}$	$9.61\cdot10^{-3}$
q_∞ [kPa]	1.54	7.24	38.72	65.0
p_∞ [Pa]	5.52	287.4	1,196.4	646.27
Re^u_∞ [m^{-1}]	$3.36\cdot10^4$	$4.52\cdot10^5$	$2.39\cdot10^6$	$2.19\cdot10^6$

Winged Reentry Vehicles vs Non-winged RV

Hirschel & Weiland (DLR), Selected Aerothermodynamic Design Problems of Hypersonic Flight Vehicles, Springer, 2009.

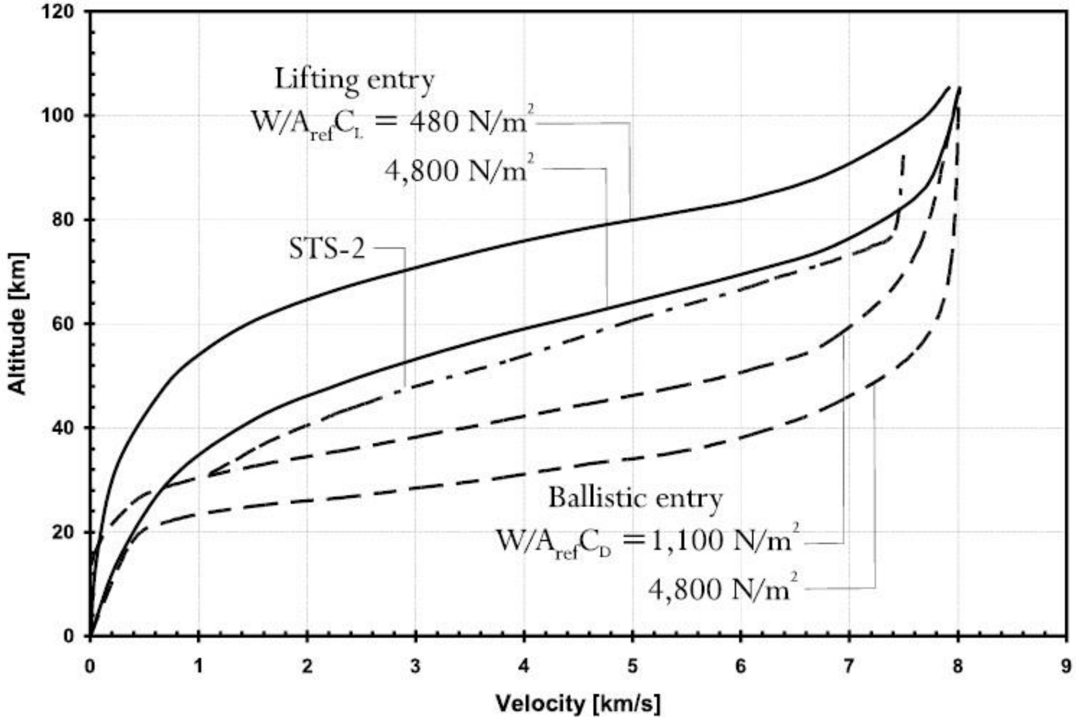

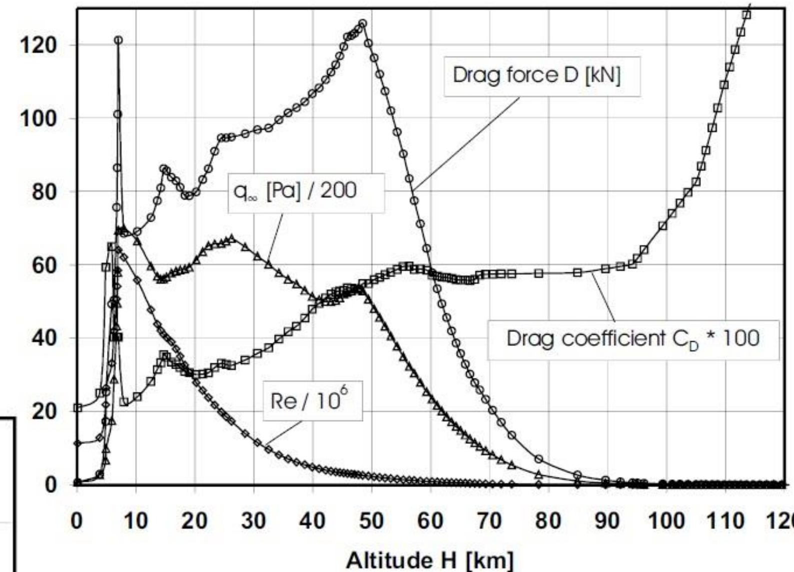

Big picture: Lifting body and control

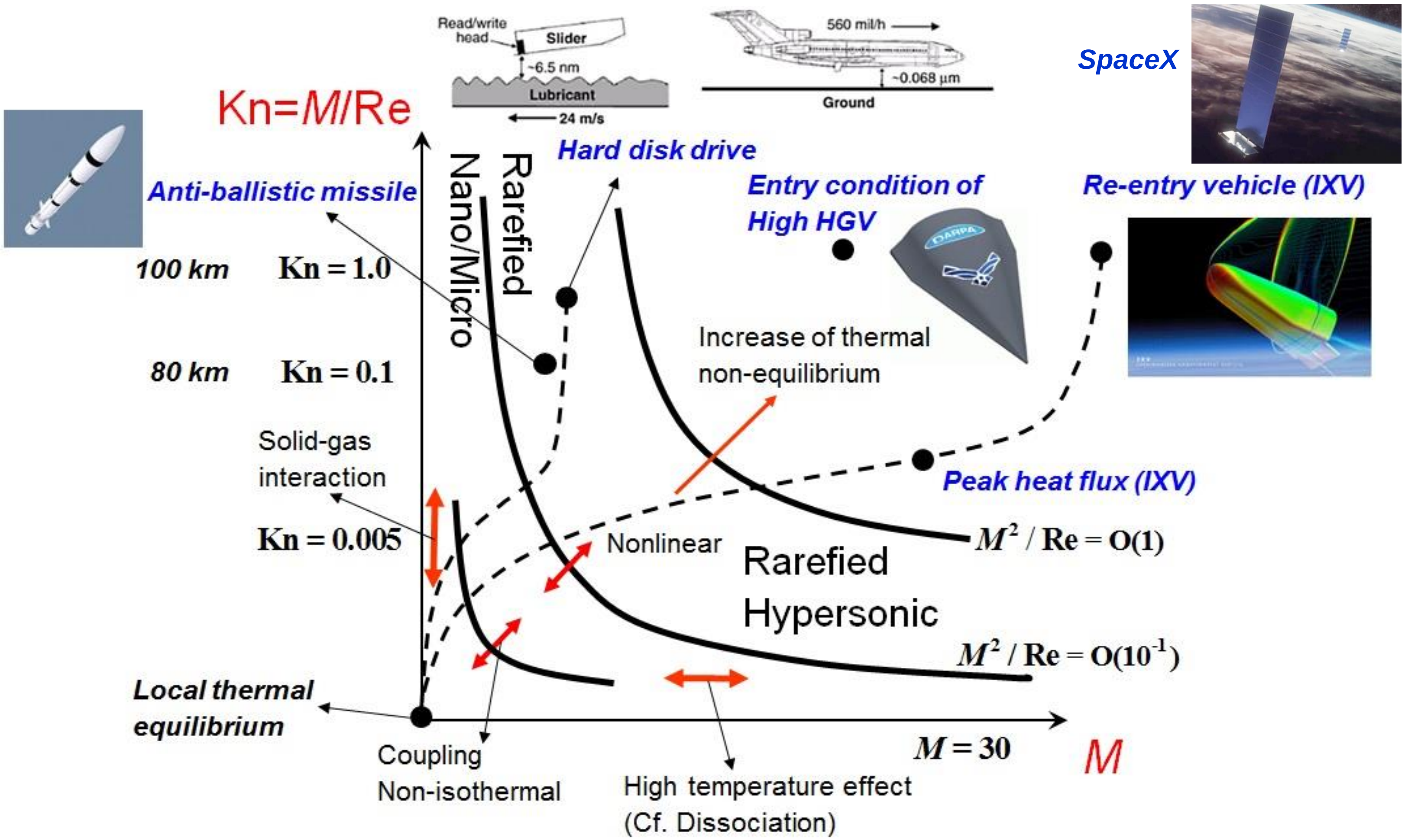

$\mathbf{v} \cdot \nabla f(\mathbf{r}, \mathbf{v}) = C[f, f_2]$ $\xrightarrow{\text{M appearing}}$ via statistical average $\rho \mathbf{u} \cdot \nabla \mathbf{u} + \nabla \cdot p\mathbf{I} + \nabla \cdot \mathbf{\Pi} = 0$ $\Longrightarrow$ **Main parameter** $\Pi / p \sim \mathrm{Kn} \cdot M$

Two terms: Kn **Three terms: *M*, Kn** **(not Kn alone)** $\dfrac{M^2}{\mathrm{Re}}$ or $\dfrac{M}{\sqrt{\mathrm{Re}}}$

Multidisciplinary Design Optimization

Pankaj Priyadarshi (Vikram Sarabhai Space Center, India), Multifidelity Multiobjective Multidisciplinary Design Optimization (M3DO) of a Semi-Ballistic Reentry Vehicle, IIT Kanpur, 2015.

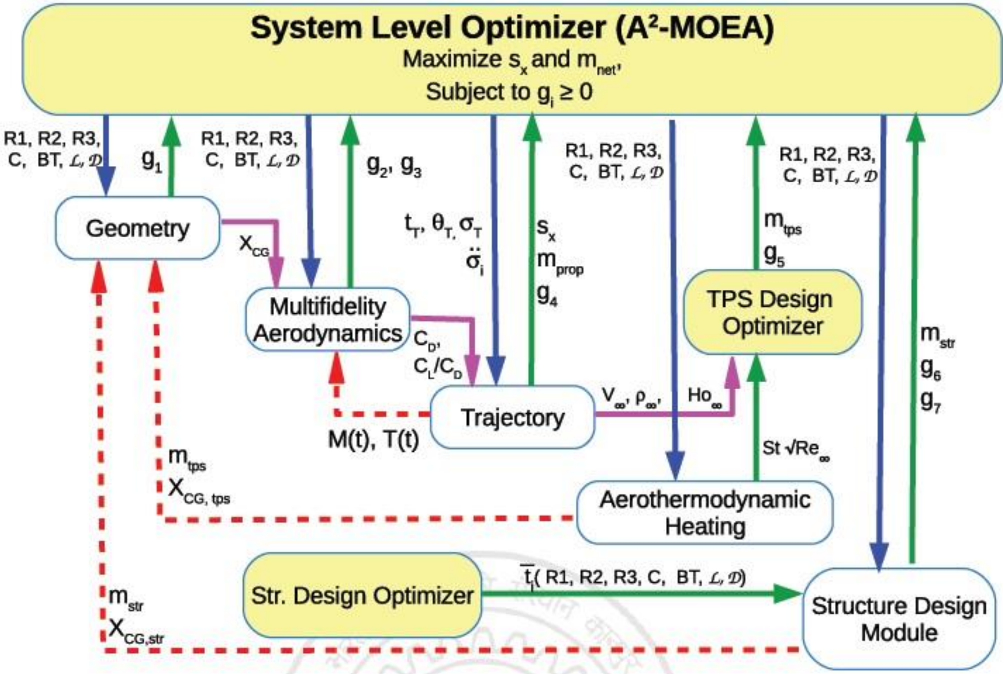

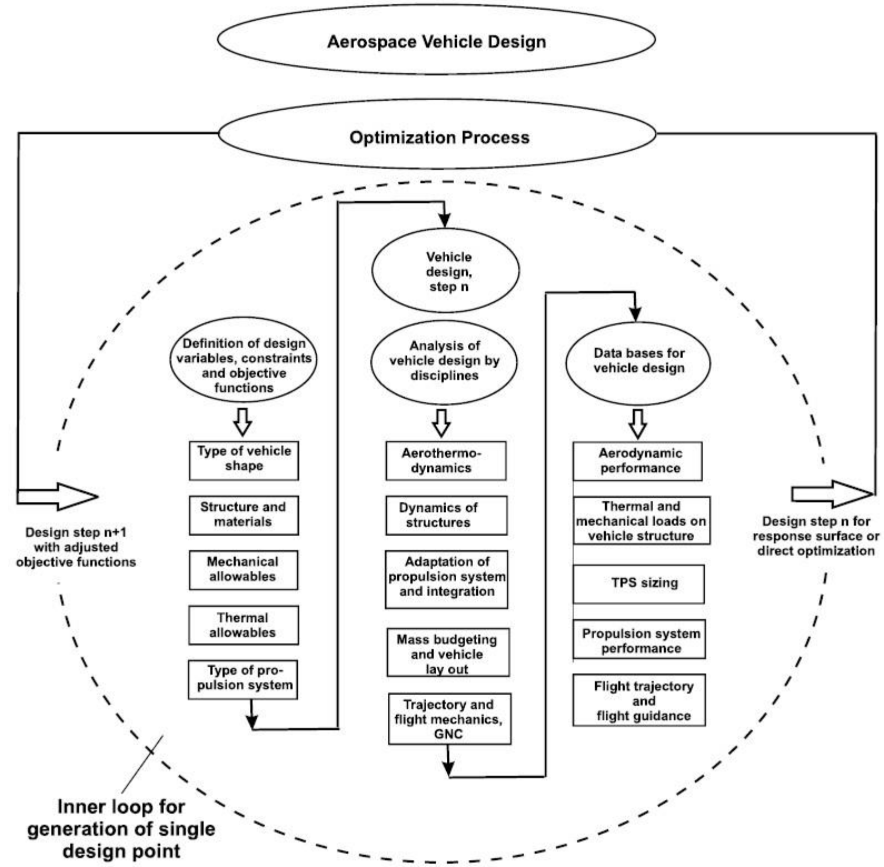

Experimental Investigation of Rarefaction Effects

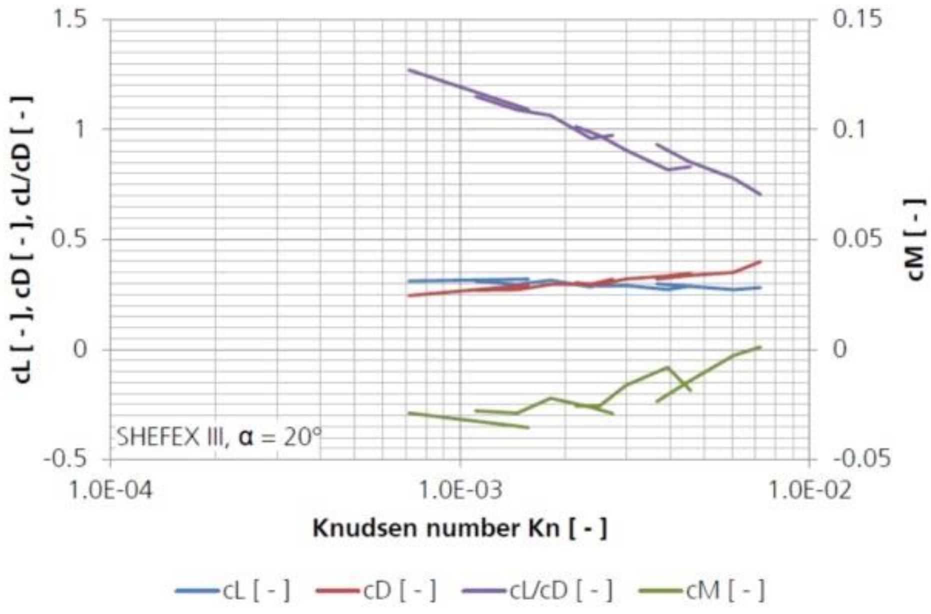

Schlegat, T., Experimental Investigation of Rarefaction Effects on Aerodynamic Coefficients of Slender and Blunt Re-entry Vehicles, Ph.D. Dissertation, Justus Liebig University, Germany, 2018.

(1) The uncertainty in heat transfer can exceed 30%, which is significantly larger than that in pressure.
(2) The heat transfer on the bottom plate relies heavily on the freestream and geometric conditions and is related to the flow structures generated by the shock waves/turbulent boundary layer interaction. High-uncertainty areas appear near the leading edge of the fin and the uncertainty near the heat flux peak is non-negligible.
(3) U_{inf}, P_{inf}, and Fin angles are top contributors to the uncertainty in heat transfer for both cases, while T_{inf} and T_{wall} show little effect.
(4) U_{inf} contributes approximately 60% to the uncertainty in heat transfer near the heat flux peak, suggesting its influence on flow reattachment.
(5) Fin angles significantly influence the aerothermal characteristics of flow separations and vortex developments. The variations of fin angles result in high uncertainties near the leading edge of fins.
(6) P_{inf} is also a key parameter for flow separation, as revealed by its high Sobol index at the separation line.

J. Lu et al., Uncertainty and sensitivity analysis of heat transfer in hypersonic three-dimensional shock waves/turbulent boundary layer interaction flows, Aerospace Science and Technology 123 (2022) 107447

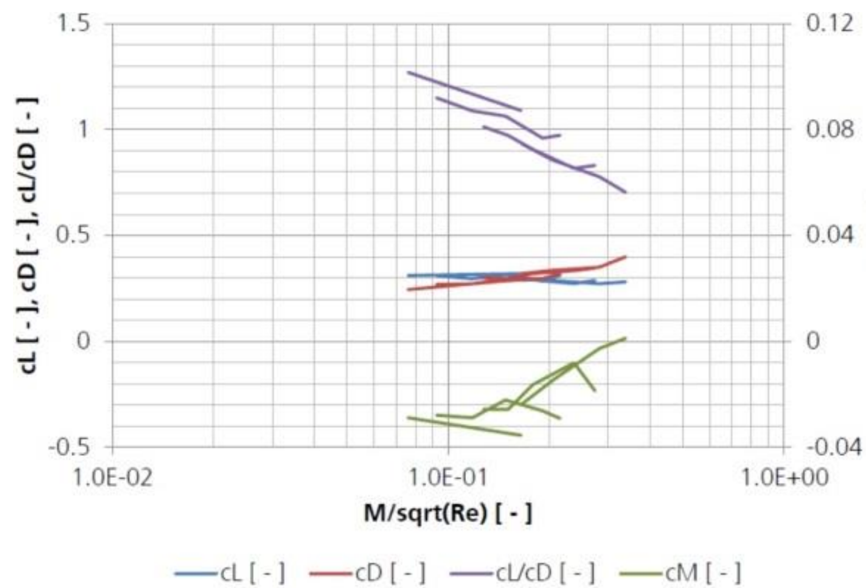

Main issues

- 우주비행기의 과학적 Mission 계속적 발굴 (국방 Mission의 경우 “우주통제”, “우주전력투사; 재사용 무인 우주비행체 고도화 기술 특화연구센터 (서울대, 2023))
- 우주비행기 해석 및 설계 핵심기술 도출 (세계 대비 독창적 기술)
- 실험과 시험에 얼마 만큼 재원 투입할 지 결정 필요

  CFD   Wind Tunnel   Flight Test   3축 체계

  에서

  CFD   Flight Test 2축 체계

  (Wind Tunnel은 시편 단위의 CFD 검증용으로만 사용하여 대용량 WT 구축/운용 절감)
- 기술적 Issues:

Pitching Moment Anomaly, 물리적/해석적 Uncertainty, 벽면의 희박(slip-jump) 효과, Thermochemical-rarefaction-radiation 복합 효과, 희박영역 추진-공력 상호작용, 효율적 Stability Derivatives 계산 등

우주 희박기체 및 우주비행기 관련 수행 연구과제

1999-03 한국과학재단 특정기초 **“**희박기체 및 **MEMS** 유동장 해석에 관한 기초연구**”**

2012-15 한국연구재단 중견연구 **“Non-classical** 열유동 물리법칙에 기초한 마이크로**-**희박 기체 연구의 새 패러다임**”**

2015-16 ADD 용역과제 **“NCCR-CFD** 기법을 이용한 연속체**-**희박 유동 통합해석 연구**” (**인하대 이승수 교수**)**

2015-18 한국연구재단 우주핵심 **“**달착륙선의 로켓플룸**-**월면 상호작용 및 표토입자 분산 연구**”**

2017-20 한국연구재단 중견연구 **“**희박·마이크로 다원자 기체와 점탄성 복잡유체에 관한 볼츠만 기반의 메조스케일 모델링 및 시스템 설계기법**”**

2017-20 우주핵심기술개발사업**(**위탁**) “**지구 재진입시 우주비행체 형상에 따른 공력가열특성 수치해석 연구**”**

2022-25 스페이스챌린지사업 **(**위탁**) “**대기 진입 시 우주비행체 보호를 위한 열 보호 시스템 개발**”**

2022-25 US Air Force Research Laboratory (AFOSR Grants) “Ultra-fast DSMC based on explainable AI for all flow regimes including rarefied hypersonics” & “Assessment of the applicability of quantum computation for solving the problem of numerical hypersonic flow”

비행체 운동학 및 공력가열 관련 수행 연구과제

2003-04 ㈜한화 **"**로켓 비행체 예비설계용 공력 예측 프로그램 개발**" (DATCOM)**

2008-09 ㈜한화 **"**카나드 제어 유도 로켓 시스템의 사거리 최적화를 위한 공력 및 항력 특성 연구**"**

2009-11 ㈜한화 **"**차기 다연장 유도 미사일 공력특성에 관한 연구**" (**천무**)**

2013-13 ㈜한화 **"**유도무기 고앙각 영역에서의 롤 안정성 향상 연구**" (**천무**)**

2018-19 LIG넥스원 **"**공력가열 및 **Plume** 적외선 신호 계산 알고리즘 위탁용역연구**"**

(Beckwith (1957), Fay & Riddell (1958), van Driest (1959) 경험식**)**

이지현 등**, KSAS, 47(11), 768-778(2019)**

Vinh-Busemann-Culp의 우주비행체 질점 모델 **(1980)**

Vinh, N. X., Busemann, A. and Culp, R. D., Hypersonic and Planetary Entry Flight Mechanics, University of Michigan Press, Ann Arbor, MI, 1980, pp. 19-28

재진입 비행체 공력가열 해석 예

Chae, J. H., Mankodi, T. K., Choi, S. M., Myong, R. S., **Combined Effects of Thermal Non-equilibrium and Chemical Reactions on Hypersonic Air Flows** Around An Orbital Reentry Vehicle, ***International Journal of Aeronautical and Space Science***, Vol. 21, pp. 612-626, **2020**.

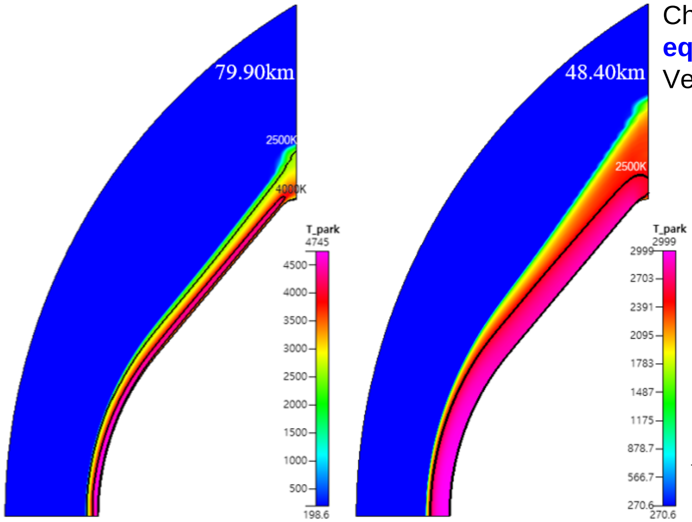

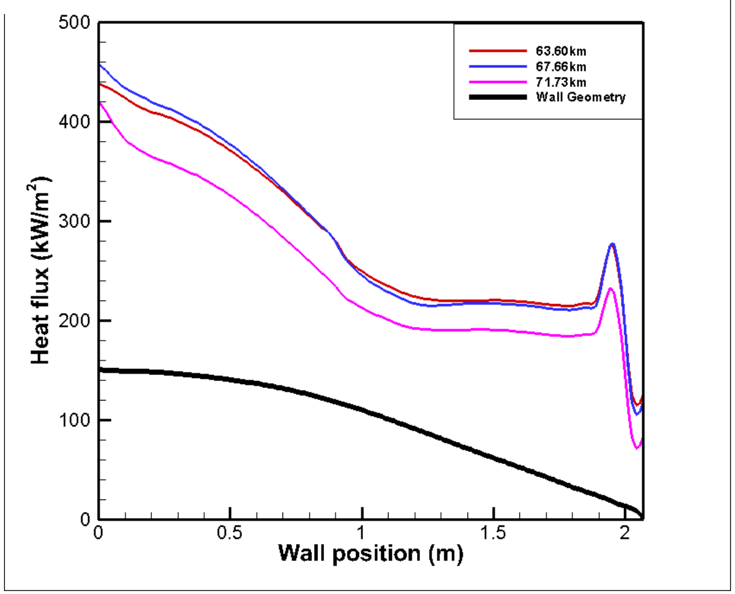

Japanese orbital reentry experiment (OREX) vehicle

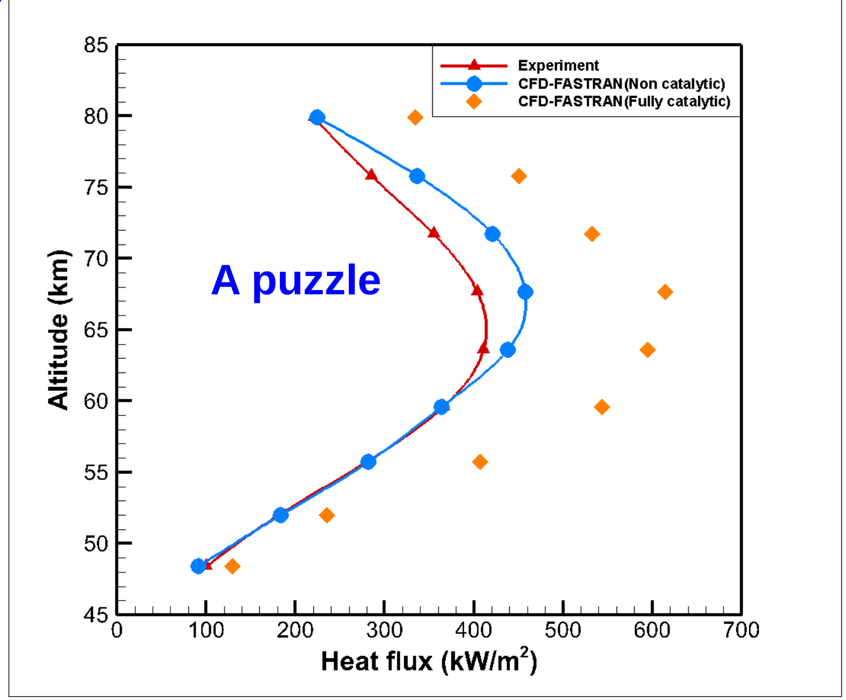

CFD-FASTRAN (US) code based on Navier-Stokes, 5-species air, Park's two-temperature model s

Plausible explanation on the puzzle

Japanese orbital reentry experiment (OREX) vehicle

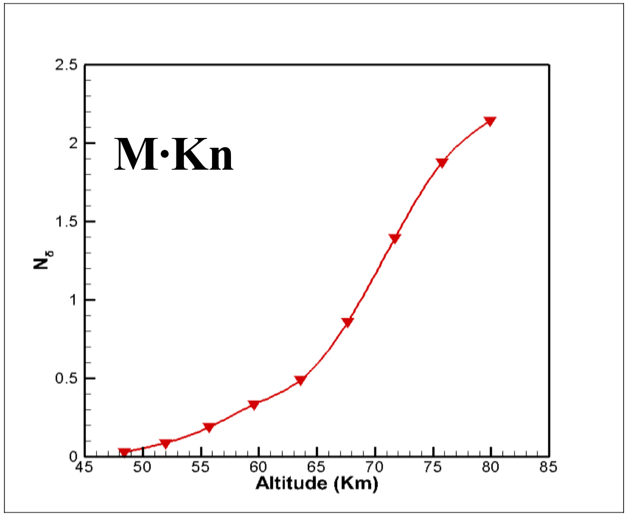

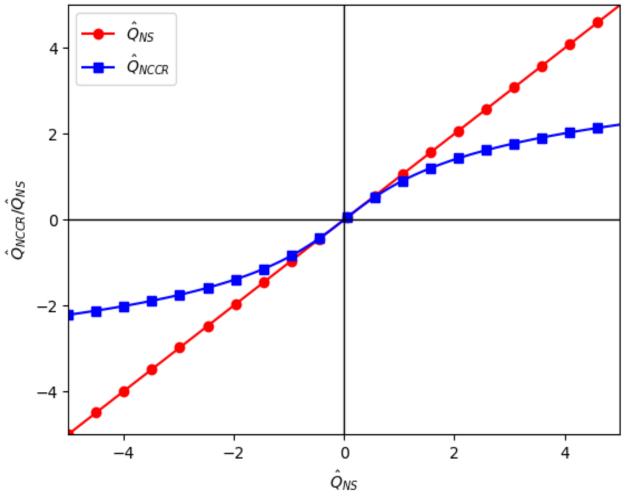

Two competing effects: the shortcoming of the first-order law of heat flux in the NSF, and the inaccurate description of the effects of thermal non-equilibrium on chemical reactions in Park's two temperature model.

The former dominates around the altitude of 70 km, while the former and latter effects cancel out at the highest altitude of 80 km, leading to an excellent match with the actual flight test data

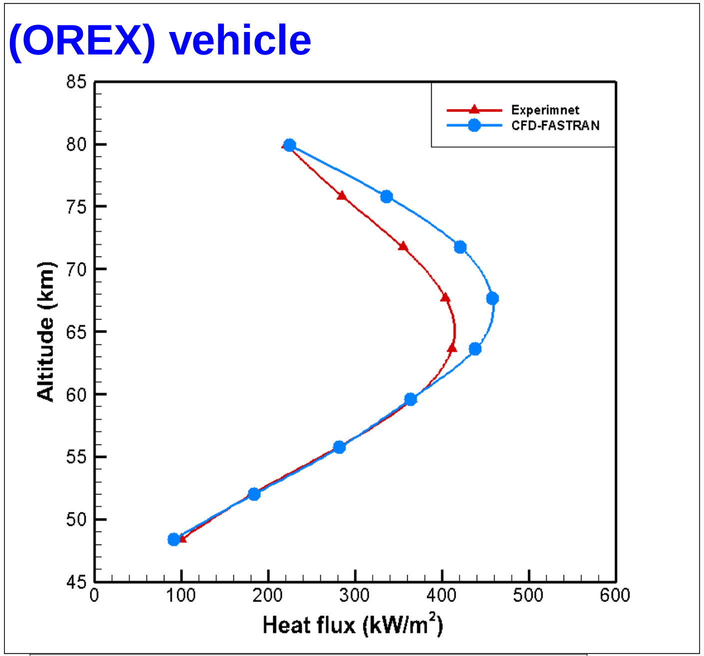

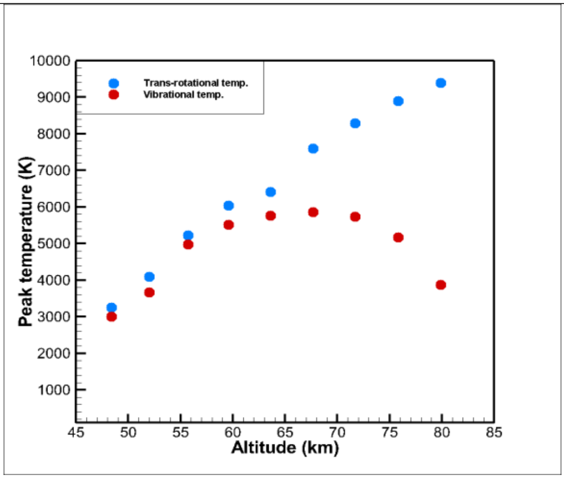

비행체 6자유도 운동 분석을 위한 공력 데이타

DATCOM Output

$$I_y \ddot{\theta} \approx q\, S\, d\, C_{m_\alpha}\, \alpha + q\, S_{Ref}\, d\, C_{m_\delta}\, \delta$$

- **Basic Output (one time run)**
  - **Center of Pressure:** $X_{C.P.}$
  - **Coefficients:** $C_{\{N,A,Y\}}, C_{\{L,D\}}, C_{\{l,m,n\}}$
  - **Primary stability derivatives:** $C_{\{N,m\}_\alpha}, C_{\{Y,l,n\}_\beta}$
  - **Secondary (damping) stability derivatives:** $C_{\{N,A,Y,l,m,n\}_{\{p,q,r\}}}, C_{\{N,m\}_{\dot{\alpha}}}$
- **Control derivatives: available by running multiple cases**
  - **Examples:** $C_{\{m,l\}_\delta}$
- **Basic Output (one time run)**

$$C_{\{N,A,Y,l,m,n\}} = \text{function}(M, \alpha, \beta, \delta, + \text{ or } \times, \text{Re}) \text{ and}$$

$$C_{\{N,A,Y,l,m,n\}} = \text{function}(p, q, r, \dot{\alpha}, \dot{\beta})$$

우주비행기 열공력모우멘트 해석 코드 현황

Commercial CFD codes base don Navier-Stokes-Fourier equations	
CFD-FASTRAN	ESI CFD, Inc. (US) Multi-species air, Park’s two-temperature chemical reaction model
CFD++	Metacomp Technologies Inc. (US) Multi-species air, Park’s two-temperature chemical reaction model

nccrFOAM suite (GNU)	**2nd-order constitutive laws with the vibrational mode (two-temperature)**

DS1V,DS2V,DS3V	**Original DSMC codes by Graeme Bird**
DAC	From Jay LeBeau's group at NASA
MGDS	From Tom Schwartzentruber's group at U Minnesota
dsmcFoam (2010) & dsmcFoam+ (2018)	OpenFoam packages developed by Scanlon et al. (C&F 39-10, pp.2078-2089, 2010) and White et al. (CPC 224, pp.22-43, 2018)
Monaco	From Iain Boyd's group at U Michigan
SMILE	From the Khristianovich Institute of Theoretical and Applied Mechanics in Russi a
PI-DSMC	Parallel version of DS2V and DS3V by Martin Rose of the PI-DSMC company
SPARTA	Stochastic PArallel Rarefied-gas Time-accurate Analyzer developed by Sandia National Laboratories

Park's two temperature model (1988)

From now on, no consideration on air-solid molecular interaction, ablation, and radiation

Average Temperature Model

In this model, the rate coefficient is assumed to be dictated by the (geometric) average temperature

$$T_a = \sqrt{T \times T_v} \qquad (10)$$

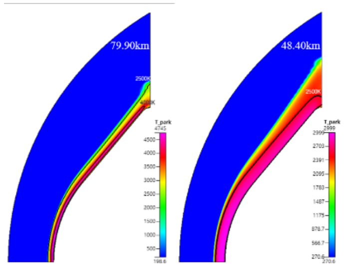

("Assessment of Two-Temperature Kinetic Model for Dissociating and Weakly-Ionizing Nitrogen," *J. of Thermophysics and Heat Transfer*, Vol. 2, pp. 8-16, 1988)

("The Limits of Two-Temperature Model," *AIAA 2010-911*: It describes what the two-temperature model is, and why it was developed. It then explains why the model is the way it is, and **what it cannot do**. It suggests a three-temperature model recognizing the rotational temperature or a radiation temperature different from heavy particle translational temperature.)

Argon **Nitrogen** **Carbon dioxide**

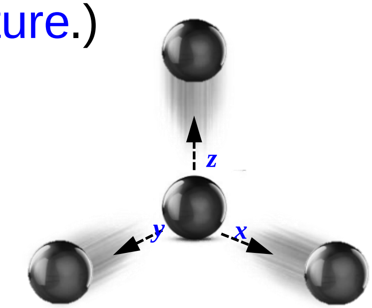

Translational degree of freedom

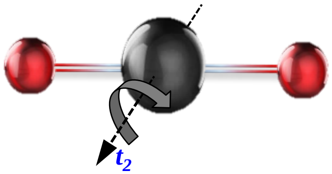

Rotational degree of freedom

NETT (Non-equilibrium Total Temperature) Model

- With the recent development of high-fidelity *ab initio* based computational chemistry algorithms, **Potential Energy Surface** information of various gas particles can be acquired using Complete Active Space Self-consistent Field (CASSCF) and Second-order Perturbation Theory (CASPT2) techniques.
- By combining this information with the **Molecular Dynamics** simulation based on the Quasi-classical Trajectory technique, the cross sections and rate coefficients of a chemical reaction can be calculated. (Luo, H., Kulakhmetov, M., and Alexeenko, A., "Ab Initio State-specific N2 + O Dissociation and Exchange Modeling for Molecular Simulations," *Journal of Chemical Physics*, Vol. 146, 074303, 2017.)
- It is crucial to realize that, although Park's two-temperature model over-predicts dissociation rates at lower vibrational temperatures, it is widely used today because of its clear and simple implementation.
- A physically-motivated model for non-equilibrium reaction rate coefficients suitable for the NSF equations is proposed. (Mankodi, T. K., Myong, R. S., Quasi-classical Trajectory-based Non-equilibrium Chemical Reaction Models for Hypersonic Air Flows, ***Physics of Fluids***, Vol. 31, 106102, **2019.)**

NETT (Non-equilibrium Total Temperature): results

$$k(T_{tr},T_v) = A\left(\frac{T_v}{T_{tr}}\right)^{\chi} T_t^{\eta} \exp\left(-\frac{D}{T_t}\right),$$

Park's model with $\alpha = 0.5$

$$\ln T_a = \alpha \ln T_{tr} + (1-\alpha)\ln T_v$$

$$T_t = \alpha T_{tr} + (1-\alpha)T_v, \quad \alpha = \frac{\delta_{tr}}{\delta_{tr}+\delta_{vib}}, \quad \delta_{tr}(=3+2)=5, \quad \delta_{vib} = \frac{2e_{vib}}{R_S T_V}, \quad e_{vib} = \frac{R_S\theta_{vib}}{\exp(\theta_{vib}/T_v)-1}$$

NETT Model

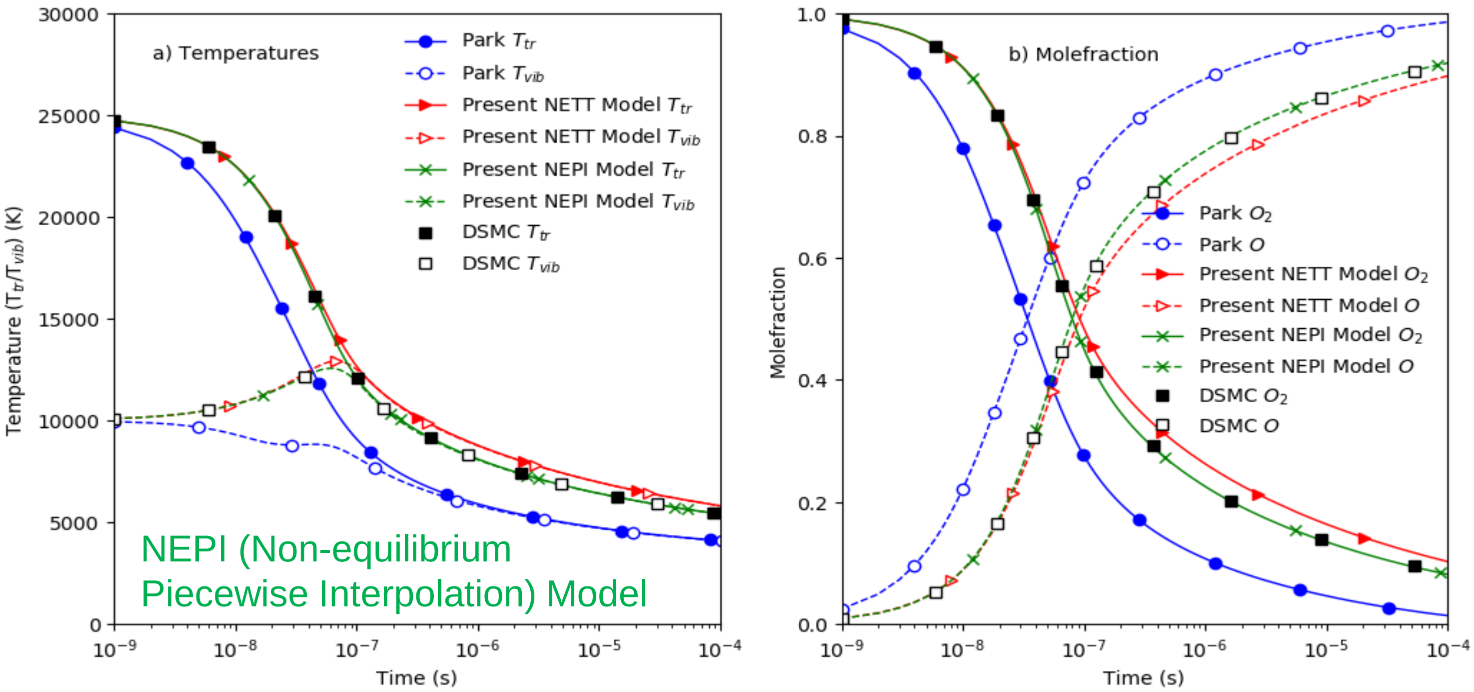

Evolution of O and O_2 for simulation starting with vibrationally cold conditions

Boltzmann kinetic equations

- A first-order partial differential equation of **the probability density of finding a particle in phase space** with an integral collision term

$$\left(\frac{\partial}{\partial t}+\mathbf{v}\cdot\nabla\right)f(t,\mathbf{r},\mathbf{v})=\frac{1}{Kn}C[f,f_2]$$

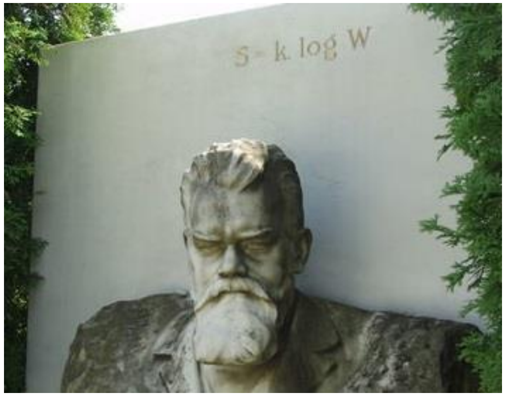

Movement — Collision (or Interaction)

Kinematic — Dissipation

$$C[f,f_2]\sim\int|\mathbf{v}-\mathbf{v}_2|(f^*f_2^*-ff_2)d\mathbf{v}_2$$

$=$ Gain (scattered into) - Loss (scattered out) $=\left(\frac{\delta f}{\delta t}\right)^{+}-\left(\frac{\delta f}{\delta t}\right)^{-}$

- **Maxwell's equation of transfer** for molecular expression $h^{(n)}$

$$\frac{\partial}{\partial t}\left\langle h^{(n)}f\right\rangle+\nabla\cdot\left(\mathbf{u}\left\langle h^{(n)}f\right\rangle+\left\langle\mathbf{c}h^{(n)}f\right\rangle\right)-\left\langle f\frac{d}{dt}h^{(n)}\right\rangle-\left\langle f\mathbf{c}\cdot\nabla h^{(n)}\right\rangle=\left\langle h^{(n)}C[f,f_2]\right\rangle$$

Relationship with conservation laws

Boltzmann transport equation (BTE): 10^{23}

$$\left(\frac{\partial}{\partial t}+\mathbf{v}\cdot\nabla\right)f(t,\mathbf{r},\mathbf{v})=C[f,f_2]$$

$$\rho\mathbf{u}=\langle m\mathbf{v}f(t,\mathbf{r},\mathbf{v})\rangle$$

where $\langle\cdots\rangle=\iiint\cdots dv_x dv_y dv_z$

Differentiating the statistical definition $\rho\mathbf{u}\equiv\langle m\mathbf{v}f(t,\mathbf{r},\mathbf{v})\rangle$ *with time* and *then combining* with BTE ($t,\mathbf{r},\mathbf{v}$ are independent and $\mathbf{v}=\mathbf{u}+\mathbf{c}$)

$$\frac{\partial}{\partial t}\langle m\mathbf{v}f\rangle=\left\langle m\mathbf{v}\frac{\partial f}{\partial t}\right\rangle=-\langle m(\mathbf{v}\cdot\nabla f)\mathbf{v}\rangle+\langle m\mathbf{v}C[f,f_2]\rangle$$

$[\mathbf{A}]^{(2)}$: Traceless symmetric part of tensor $\mathbf{A}$

Here $-\langle m(\mathbf{v}\cdot\nabla f)\mathbf{v}\rangle=-\nabla\cdot\langle m\mathbf{v}\mathbf{v}f\rangle=-\nabla\cdot\{\rho\mathbf{u}\mathbf{u}+\langle m\mathbf{c}\mathbf{c}f\rangle\}$

After the decomposition of the stress into pressure and viscous shear stress

$\mathbf{P}\equiv\langle m\mathbf{c}\mathbf{c}f\rangle=p\mathbf{I}+\mathbf{\Pi}$ where $p\equiv\langle m\mathrm{Tr}(\mathbf{c}\mathbf{c})f/3\rangle$, $\mathbf{\Pi}\equiv\langle m[\mathbf{c}\mathbf{c}]^{(2)}f\rangle$,

and using the collisional invariance of the momentum, $\langle m\mathbf{v}C[f,f_2]\rangle=0$, we have

$$\frac{\partial(\rho\mathbf{u})}{\partial t}+\nabla\cdot(\rho\mathbf{u}\mathbf{u}+p\mathbf{I}+\mathbf{\Pi})=0$$

Conservation laws: 13

PHYSICAL REVIEW E VOLUME 56, NUMBER 3 SEPTEMBER 1997

Generalized hydrodynamics and shock waves

Mazen Al-Ghoul and Byung Chan Eu*
Department of Chemistry, McGill University, 801 Sherbrooke Street West, Montreal, Quebec, Canada H3A 2K6
(Received 6 December 1996; revised manuscript received 3 March 1997)

Constitutive equations and balanced closure

Conceptual inconsistency of Eu's closure (B. C. Eu 1992)

$$\langle m\mathbf{cccf}\rangle - \langle m\mathrm{Tr}(\mathbf{ccc})f\rangle \mathbf{I}/3 = 0 \;\Rightarrow\; \text{Vanishing heat flux}$$

$$\langle m\mathbf{cccf}\rangle = 0 \;\Rightarrow\; \text{Cannot be zero in general}$$

New balanced closure with closure-last approach (PoF 2014)

2nd-order for kinematic LH = 2nd-order for collsion RH

2nd-order closure

$$\rho\frac{D}{Dt}\begin{bmatrix}\mathbf{\Pi}\left(\equiv\langle m[\mathbf{cc}]^{(2)}f\rangle\right)/\rho \\ \mathbf{Q}\left(\equiv\langle mc^2\mathbf{c}/2f\rangle\right)/\rho\end{bmatrix}+\nabla\cdot\begin{bmatrix}\langle m\mathbf{cccf}\rangle-\langle m\mathrm{Tr}(\mathbf{ccc})f\rangle\mathbf{I}/3 \\ \langle mc^2\mathbf{cc}f/2\rangle - C_pT(p\mathbf{I}+\mathbf{\Pi})\end{bmatrix}+\begin{bmatrix}0 \\ \langle m\mathbf{cccf}\rangle:\nabla\mathbf{u}\end{bmatrix}$$

$$\begin{bmatrix}2[\mathbf{\Pi}\cdot\nabla\mathbf{u}]^{(2)} \\ \frac{D\mathbf{u}}{Dt}\cdot\mathbf{\Pi}+\mathbf{Q}\cdot\nabla\mathbf{u}+\mathbf{\Pi}\cdot C_p\nabla T\end{bmatrix}+\begin{bmatrix}2p[\nabla\mathbf{u}]^{(2)} \\ pC_p\nabla T\end{bmatrix}=\begin{bmatrix}\langle m[\mathbf{cc}]^{(2)}C[f,f_2]\rangle \\ \langle\left(mc^2/2-mC_pT\right)\mathbf{c}C[f,f_2]\rangle\end{bmatrix}$$

2nd-order closure

Closure of dissipation terms via 2nd-law

Key ideas; exponential canonical form, consideration of entropy production σ, and non-polynomial expansion called as cumulant expansion (B. C. Eu in 80-90s)

(2007)

By writing the distribution function f in the exponential form

$$f = \exp\left[-\beta\left(\frac{1}{2}mc^2 + \sum_{n=1}^{\infty} X^{(n)} h^{(n)} - N\right)\right],\ \beta \equiv \frac{1}{k_B T},$$

Nonequilibrium entropy Ψ : $\Psi(\mathbf{r},t) = -k_B \left\langle \left[\ln f(\mathbf{v},\mathbf{r},t) - 1\right] f(\mathbf{v},\mathbf{r},t) \right\rangle,$

Nonequilibrium entropy production: $\sigma_c \equiv -k_B \left\langle \ln f \ C[f, f_2] \right\rangle \geq 0$ (satisfying 2nd-law)

$\sigma_c = \kappa_1 q(\kappa_1^{(\pm)}, \kappa_2^{(\pm)}, \cdots)$ via cumulant expansion

$$\sigma_c \equiv -k_B \left\langle \ln f \ C[f, f_2] \right\rangle = \frac{1}{T}\sum_{n=1}^{\infty} X^{(n)} \left\langle h^{(n)} C[f, f_2] \right\rangle = \frac{1}{T}\sum_{l=1}^{\infty} X^{(n)} \Lambda^{(n)},$$

a thermodynamically-consistent constitutive equation, still exact to BKE, can be derived;

$$\rho \frac{D(\mathbf{\Pi}/\rho)}{Dt} + \nabla \cdot \mathbf{\Psi}^{(\Pi)} + 2\left[\mathbf{\Pi} \cdot \nabla \mathbf{u}\right]^{(2)} + 2p\left[\nabla \mathbf{u}\right]^{(2)} = \frac{1}{\beta g}\sum_{l=1}^{\infty} R_{12}^{(2l)} X_2^{(l)} q(\kappa_1^{(\pm)}, \kappa_2^{(\pm)}, \cdots)$$

Cumulant expansion method

$$\langle x^l \rangle = \int x^l f(x)dx, \quad \langle e^{\lambda x} \rangle = \int e^{\lambda x} f(x)dx$$

Then we have

$$\langle e^{\lambda x} \rangle = \sum_{l=0}^{\infty} \frac{\lambda^l}{l!} \langle x^l \rangle = \exp\left[\sum_{l=1}^{\infty} \frac{\lambda^l}{l!} \kappa_l\right] \text{ where}$$

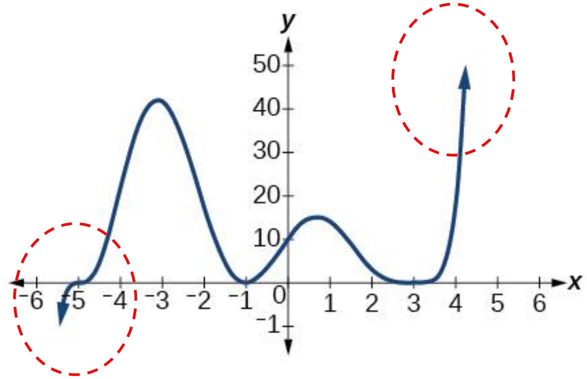

$$\kappa_l = \left[\frac{d^l}{d\lambda^l} \ln \langle e^{\lambda x} \rangle\right]_{\lambda=0} ; \; \kappa_1 = \langle x \rangle, \; \kappa_2 = \langle x^2 \rangle - \langle x \rangle^2, \cdots \text{ (mean, variance)}$$

$$\langle e^x \rangle_{\text{polynomical}} = 1 + \langle x \rangle + \frac{1}{2!}\langle x^2 \rangle + \frac{1}{3!}\langle x^3 \rangle + \cdots,$$

$$\langle e^x \rangle_{\text{cumulant}} = \exp^{\left[\langle x \rangle + \frac{1}{2!}\left(\langle x^2 \rangle - \langle x \rangle^2\right) + \cdots\right]}$$

$$\left(\langle e^x \rangle - \langle e^{-x} \rangle\right)/2\Big]_{\text{polynomial}} = \langle x \rangle + \frac{1}{3}\langle x^3 \rangle + \cdots \approx \langle x \rangle$$

$$\left(\langle e^x \rangle - \langle e^{-x} \rangle\right)/2\Big]_{\text{cumulant}} = \exp^{\left(\frac{1}{2!}\left(\langle x^2 \rangle - \langle x \rangle^2\right) + \cdots\right)} \left[\exp^{\left(\langle x \rangle + \cdots\right)} - \exp^{\left(-\langle x \rangle + \cdots\right)}\right] / 2 \underset{2nd}{\approx} \sinh \langle x \rangle$$

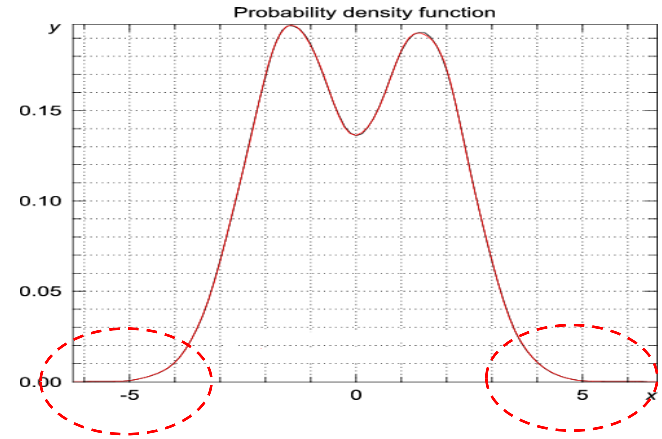

2nd-order NCCR model

NCCR: Nonlinear Coupled Constitutive Relation

Conservation laws (exact consequence of BKE)

$$\frac{\partial(\rho\mathbf{u})}{\partial t}+\nabla\cdot\left(\rho\mathbf{uu}+p\mathbf{I}+\mathbf{\Pi}\right)=\mathbf{0}$$

in conjunction with the 2nd-order constitutive relations (CR)

Zero in 2nd-order approximation

$$\frac{\partial\mathbf{\Pi}}{\partial t}+\mathbf{u}\cdot\nabla\mathbf{\Pi}+\nabla\cdot\left(\langle m\mathbf{ccc}f\rangle-\langle m\mathrm{Tr}(\mathbf{ccc})f\rangle\mathbf{I}/3\right)$$

Non-local term

$$+2\left[\mathbf{\Pi}\cdot\nabla\mathbf{u}\right]^{(2)}+2p\left[\nabla\mathbf{u}\right]^{(2)}=-\frac{p}{\mu_{NS}}\mathbf{\Pi}q_{2nd}(\kappa_1)$$

2nd-order coupling — Navier 1st law

$$q_{2nd}(\kappa_1)\equiv\frac{\sinh\kappa_1}{\kappa_1},\quad \kappa_1\equiv\frac{T^{1/4}}{p}\left(\frac{\mathbf{\Pi}:\mathbf{\Pi}}{\mu_{NS}}+\frac{\mathbf{Q}\cdot\mathbf{Q}/T}{k_{NS}}\right)^{1/2}$$

Onsager-Rayleigh dissipation function

Can be used as a breakdown parameter in CFD-DSMC hybrid scheme

2nd-order theory

1st-order theory

Sinh{1st-order theory}

Navier-Fourier laws inclusive like onion!

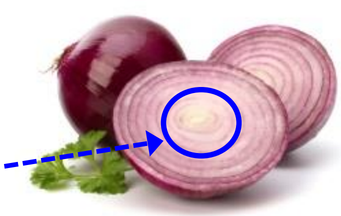

Topology of 2nd-order NCCR (shock structure) (PoF 2020a)

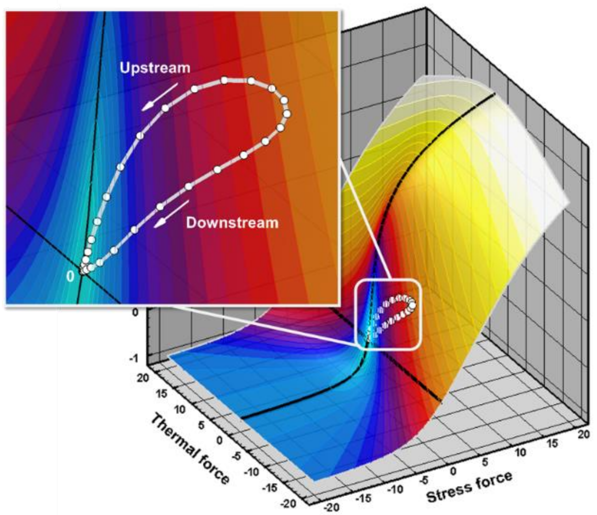

f_b=0.0

Mach 5.0

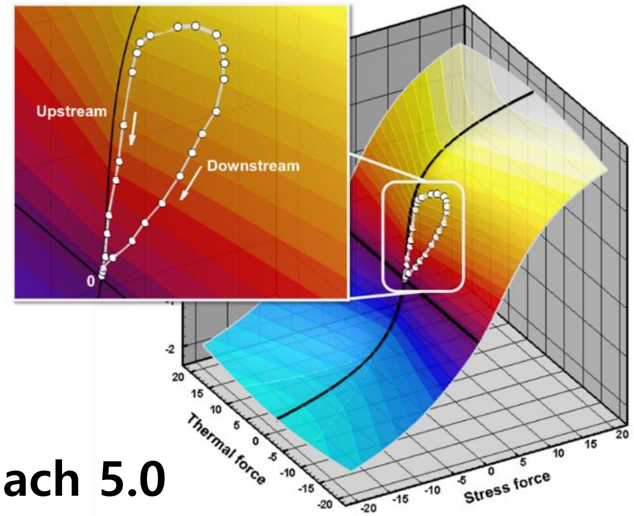

f_b=0.8

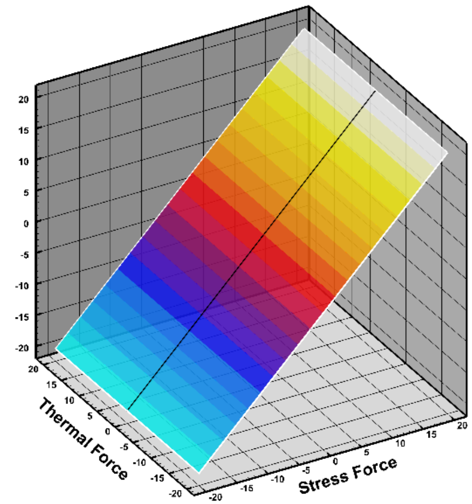

1st-order

$$\left[\hat{\mathbf{\Pi}}\cdot\nabla\hat{\mathbf{u}}\right]^{(2)} + \left(1+f_b\hat{\Delta}\right)\hat{\mathbf{\Pi}}_0 = \hat{\mathbf{\Pi}}q_{2nd}(c\hat{R}), \quad \text{(shear stress)}$$

$$\frac{3}{2}\left(\hat{\mathbf{\Pi}}+f_b\hat{\Delta}\mathbf{I}\right):\nabla\hat{\mathbf{u}} + \hat{\Delta}_0 = \hat{\Delta}q_{2nd}(c\hat{R}), \quad \text{(excess normal stress)}$$

$$\hat{\mathbf{\Pi}}\cdot\hat{\mathbf{Q}}_0 + \left(1+f_b\hat{\Delta}\right)\hat{\mathbf{Q}}_0 = \hat{\mathbf{Q}}q_{2nd}(c\hat{R}), \quad \text{(heat flux)}$$

$$\hat{\mathbf{\Pi}}_0 = -2\mu[\nabla\mathbf{u}]^{(2)}$$

$$\hat{\Delta}_0 = -\mu_b\nabla\cdot\mathbf{u}$$

$$\hat{\mathbf{Q}}_0 = -k\nabla T$$

where $\hat{R}^2 \equiv \hat{\mathbf{\Pi}}:\hat{\mathbf{\Pi}} + (5-3\gamma)f_b\hat{\Delta}^2 + \hat{\mathbf{Q}}\cdot\hat{\mathbf{Q}}$ (Onsager-Rayleigh dissipation function)

$$\Delta = \left\langle m\mathrm{Tr}(\mathbf{cc})f/3 - m\mathrm{Tr}(\mathbf{cc})f^{(0)}/3\right\rangle,\ p = \left\langle m\mathrm{Tr}(\mathbf{cc})f^{(0)}/3\right\rangle$$

Topology of 2nd-order NCCR (velocity shear) (PoF 2020a)

Carbon dioxide

Analogy among the second-order constitutive model, orbits of planets and comets, and Dirac cones.

	Second-order constitutive model in diatomic and polyatomic gases	Motion of the planets and comets in the two-body Kepler problem
Form of conic sections	$\left(1-\frac{9}{2}f_b^2\right)x^2+x+\frac{2}{3}y^2=0$ $f_b=\frac{\text{bulk viscosity}}{\text{shear viscosity}}$	$\left(1-e^2\right)x^2+2epx+y^2-p=0$ $p=\frac{L^2}{Gm_1^2m_2^2/(m_1+m_2)}$ L: angular momentum G: gravitational constant $m_{1,2}$: mass $E_{\min}=-\frac{G^2m_1^3m_2^3/(m_1+m_2)}{2L}$
Definition of x and y	$x=\frac{\Pi_{xx}}{p},\quad y=\frac{\Pi_{xy}}{p}$	$x=r\cos\theta,\ y=r\sin\theta$
Eccentricity	$e=\sqrt{\frac{27}{4}f_b^2-\frac{1}{2}}$, for $f_b\geq\sqrt{6}/9$	$e=\sqrt{1-\frac{E}{E_{\min}}}$, for $E\geq E_{\min}(<0)$
Topological properties	$f_b=\sqrt{6}/9$; $e=0$ (circle), $\sqrt{6}/9<f_b<\sqrt{2}/3$; $0<e<1$ (ellipse), $f_b=\sqrt{2}/3$; $e=1$ (parabola), $f_b>\sqrt{2}/3$; $e>1$ (hyperbola)	$E=E_{\min}$; $e=0$ (circle), $E_{\min}<E<0$; $0<e<1$ (ellipse), $E=0$; $e=1$ (parabola), $E>0$; $e>1$ (hyperbola)
Direct analogy	$f_b\Leftrightarrow\frac{2\sqrt{3}}{9}\sqrt{\frac{1}{2}+e}=\frac{\sqrt{6}}{9}\sqrt{3-\frac{2E}{E_{\min}}}$ $f_b=0.2722\Leftrightarrow e_{\text{Earth}}=0.0167$, $f_b=0.2834\Leftrightarrow e_{\text{Mercury}}=0.2056$, $f_b=0.4611\Leftrightarrow e_{\text{Halley}}=0.967$	

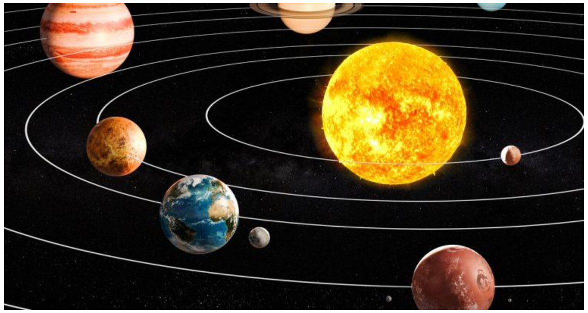

Role of the vibrational mode: Modified Boltzmann-Curtiss

$$\frac{\partial f_i}{\partial t} + \mathbf{v}\cdot\nabla f_i + \mathbf{L}\cdot\nabla_r f_i = \sum_j \sum_k \sum_l \int dv_j \int d\Omega W(i, j, | k^*, l^*; \Omega)(f_k^* f_l^* - f_i f_j)$$

$$= \sum_j C[f_i\ , f_j\ ].$$

$$a(i) + a(j) \rightarrow a(k) + a(l)$$

	Previous first-order NSF	New second-order NCCR
ρ	$\frac{\partial \rho}{\partial t} + \nabla\cdot(\rho\mathbf{u}) = 0$	$\frac{\partial \rho}{\partial t} + \nabla\cdot(\rho\mathbf{u}) = 0$
$\rho\mathbf{u}$	$\frac{\partial(\rho\mathbf{u})}{\partial t} + \nabla\cdot(\rho\mathbf{uu} + p\mathbf{I}) + \nabla\cdot\mathbf{\Pi} = 0$	$\frac{\partial(\rho\mathbf{u})}{\partial t} + \nabla\cdot(\rho\mathbf{uu} + p\mathbf{I}) + \nabla\cdot(\mathbf{\Pi} + \Delta\mathbf{I}) = 0$
ρe	$\frac{\partial(\rho e)}{\partial t} + \nabla\cdot((\rho e + p)\mathbf{u}) + \nabla\cdot(\mathbf{\Pi}\cdot\mathbf{u}) + \nabla\cdot\mathbf{Q} + \nabla\cdot\mathbf{Q}_v = 0$	$\frac{\partial(\rho e)}{\partial t} + \nabla\cdot((\rho e + p)\mathbf{u}) + \nabla\cdot((\mathbf{\Pi} + \Delta\mathbf{I})\cdot\mathbf{u}) + \nabla\cdot\mathbf{Q} + \nabla\cdot\mathbf{Q}_v = 0$
ρe_v	$\frac{\partial(\rho e_v)}{\partial t} + \nabla\cdot(\rho e_v\mathbf{u}) + \nabla\cdot\mathbf{Q}_v = \frac{\rho e_v(T_v) - \rho e_v(T)}{\tau_v}$	$\frac{\partial(\rho e_v)}{\partial t} + \nabla\cdot(\rho e_v\mathbf{u}) + \nabla\cdot\mathbf{Q}_v = \frac{\rho e_v(T_v) - \rho e_v(T)}{\tau_v}$
$\mathbf{\Pi}$	$\mathbf{\Pi} = -2\mu[\nabla\mathbf{u}]^{(2)}$	$2[\mathbf{\Pi}\cdot\nabla\mathbf{u}]^{(2)} + 2(p+\Delta)[\nabla\mathbf{u}]^{(2)} = -\frac{p}{\mu}\mathbf{\Pi}q_{2\text{nd}}(\kappa)$
Δ	$\Delta = 0$	$2\gamma'(\mathbf{\Pi} + \Delta\mathbf{I}) : \nabla\mathbf{u} + \frac{2}{3}\gamma' p\nabla\cdot\mathbf{u} = -\frac{2}{3}\gamma'\frac{p}{\mu_b}\Delta q_{2\text{nd}}(\kappa)$
$\mathbf{Q}$	$\mathbf{Q} = -k\nabla T$	$\mathbf{\Pi}\cdot\nabla(C_pT) + (p+\Delta)\nabla(C_pT) = -\frac{pC_p}{k}\mathbf{Q}q_{2\text{nd}}(\kappa)$
$\mathbf{Q}_v$	$\mathbf{Q}_v = -k_v\nabla T_v$	$\mathbf{\Pi}\cdot\nabla(C_{p,v}T_v) + (p+\Delta)\nabla(C_{p,v}T_v) = -\frac{pC_{p,v}}{k_v}\mathbf{Q}q_{2\text{nd}}(\kappa)$
$q(\kappa)$	$q_{1\text{st}}(\kappa) = 1$	$q_{2\text{nd}}(\kappa) = \frac{\sinh\kappa}{\kappa}$

PoF 2020b

$$\hat{R}^2 \equiv \hat{\mathbf{\Pi}} : \hat{\mathbf{\Pi}} + (5 - 3\gamma) f_b \hat{\Delta}^2 + \hat{\mathbf{Q}}\cdot\hat{\mathbf{Q}} + \boxed{\hat{\mathbf{Q}}_v\cdot\hat{\mathbf{Q}}_v}$$

3D mixed modal DG method for the 2nd-order model

$$\partial_t \mathbf{U} + \nabla \mathbf{F}_{\mathrm{inv}}(\mathbf{U}) + \nabla \mathbf{F}_{\mathrm{vis}}(\mathbf{U}, \nabla \mathbf{U}) = 0$$

Discretization in mixed form

$$\begin{cases} \mathbf{S} - \nabla \mathbf{U} = 0 \\ \partial_t \mathbf{U} + \nabla \mathbf{F}_{\mathrm{inv}}(\mathbf{U}) + \nabla \mathbf{F}_{\mathrm{vis}}(\mathbf{U}, \mathbf{S}) = 0 \end{cases}$$

JCP 2022

NSF model $(\boldsymbol{\Pi}, \mathbf{Q}) = \mathbf{f}_{\mathbf{linear}}(\mathbf{S}(\mathbf{U}))$

NCCR model $(\boldsymbol{\Pi}, \mathbf{Q})_{\mathbf{NCCR}} = \mathbf{f}_{\mathbf{non\text{-}linear}}(\mathbf{S}(\mathbf{U}), p, T)$

NCCR: Nonlinear Coupled Constitutive Relation

$$\mathbf{U}_h(\mathbf{x}, t) = \sum_{i=0}^{k} U_j^i(t)\varphi^i(\mathbf{x}), \quad \mathbf{S}_h(\mathbf{x}, t) = \sum_{i=0}^{k} S_j^i(t)\varphi^i(\mathbf{x})$$

$$\begin{cases} \dfrac{\partial}{\partial t}\displaystyle\int_I \mathbf{U}\varphi dV - \int_I \nabla\varphi \mathbf{F}_{\mathrm{inv}} dV + \int_{\partial I} \varphi \mathbf{F}_{\mathrm{inv}} \cdot \mathbf{n} d\Gamma - \int_I \nabla\varphi \mathbf{F}_{\mathrm{vis}} dV + \int_{\partial I} \varphi \mathbf{F}_{\mathrm{vis}} \cdot \mathbf{n} d\Gamma = 0, \\ \displaystyle\int_I \mathbf{S}\varphi dV + \int_I T^s \nabla\varphi \mathbf{U} dV - \int_{\partial I} T^s \varphi \mathbf{U} \cdot \mathbf{n} d\Gamma = 0, \end{cases}$$

Dubiner basis function, Lax-Friedrichs inviscid flux, central flux for viscous terms

Velocity-slip and temperature-jump conditions

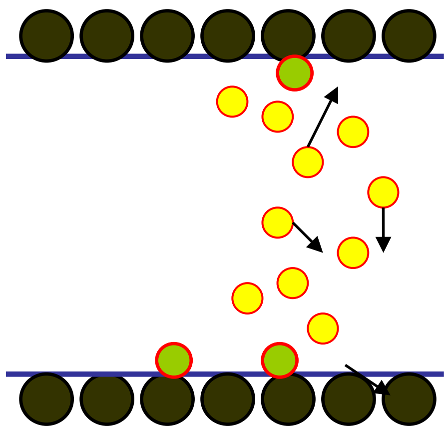

Boltzmann (or similar) in bulk flow

Gas-surface atom interaction

$$\frac{2-\sigma_v}{\sigma_v} \sim \exp\left(-\frac{D_e}{k_B T_w}\right)$$

Nonlinear Coupled

Kn*M

Morphing

(Seamless transition)

Nonlinear Coupled

Kn or Kn*M for moving wall

$$u(h/2) = V + \sigma_{V_C} l \cdot (-) \frac{\partial u}{\partial y}\bigg]_{h/2} - \frac{3}{4}\frac{\eta}{\rho T}\frac{\partial T}{\partial x}\bigg]_{h/2} \text{ and } T(h/2) = T_w + \sigma_{T_C} l \cdot (-)\frac{2\gamma}{\gamma+1}\frac{1}{\Pr}\frac{\partial T}{\partial y}\bigg]_{h/2}, \tag{2.5}$$

where $l, \sigma_{V_C}, \sigma_{T_C}$ represent the mean free path and the slip and jump constants, respectively. They were obtained after the degree of non-equilibrium is taken as *linear* with the first-order accuracy, from the following original *nonlinear coupled* models in which the velocity slip and temperature jump are determined proportionally by the degree of non-equilibrium near the wall surface,[19,35]

$$u(h/2) = V + \sigma_V l \cdot \frac{\Pi}{\eta}\bigg]_{h/2} + \sigma_{VT}\frac{3}{4}\frac{(\gamma-1)}{\gamma/\Pr}\frac{Q_x}{p}\bigg]_{h/2} \text{ and } T(h/2) = T_w + \sigma_T l \cdot \frac{2\gamma}{\gamma+1}\frac{1}{\Pr}\frac{Q_y}{k}\bigg]_{h/2}, \tag{2.6}$$

where $\sigma_V, \sigma_{VT}, \sigma_T$ represent the slip, thermal creep, and jump coefficients, respectively. But, in this work, a new idea is further introduced such that the coefficients, in particular, the thermal coefficients, are not necessarily constant and are allowed to vary with respect to the degree of non-equilibrium near the surface in the case of second-order approximation, for example, $\sigma_T = \sigma_{T_C}(1 + M \cdot \mathrm{Kn})$. Using these new nonlinear coupled velocity slip and temperature jump models, a seamless combination of two nonlinearities and couplings—NCCR for bulk flow and nonlinear coupled boundary conditions at the wall—can be achieved, as illustrated in Fig. 1, leading to the second-order constitutive and wall boundary models for velocity shear gas flow.

$$\mathbf{u}_{\text{slip}} - \mathbf{u}_{\text{wall}} = -\left(\frac{2-\sigma_v}{\sigma_v}\right)\frac{\lambda_{\text{mean}}}{\mu}\mathbf{\Pi}_{\tan} - \frac{3}{4}\frac{\Pr(\gamma-1)}{\gamma p}\mathbf{Q}_{\tan}$$

$$\mathbf{\Pi}_{\tan} = (\mathbf{n}\cdot\mathbf{\Pi})\cdot\mathbf{S}, \quad \mathbf{Q}_{\tan} = \mathbf{Q}\cdot\mathbf{S}$$

in general coordinates at the surface

2-D hypersonic rarefied flow past a cylinder

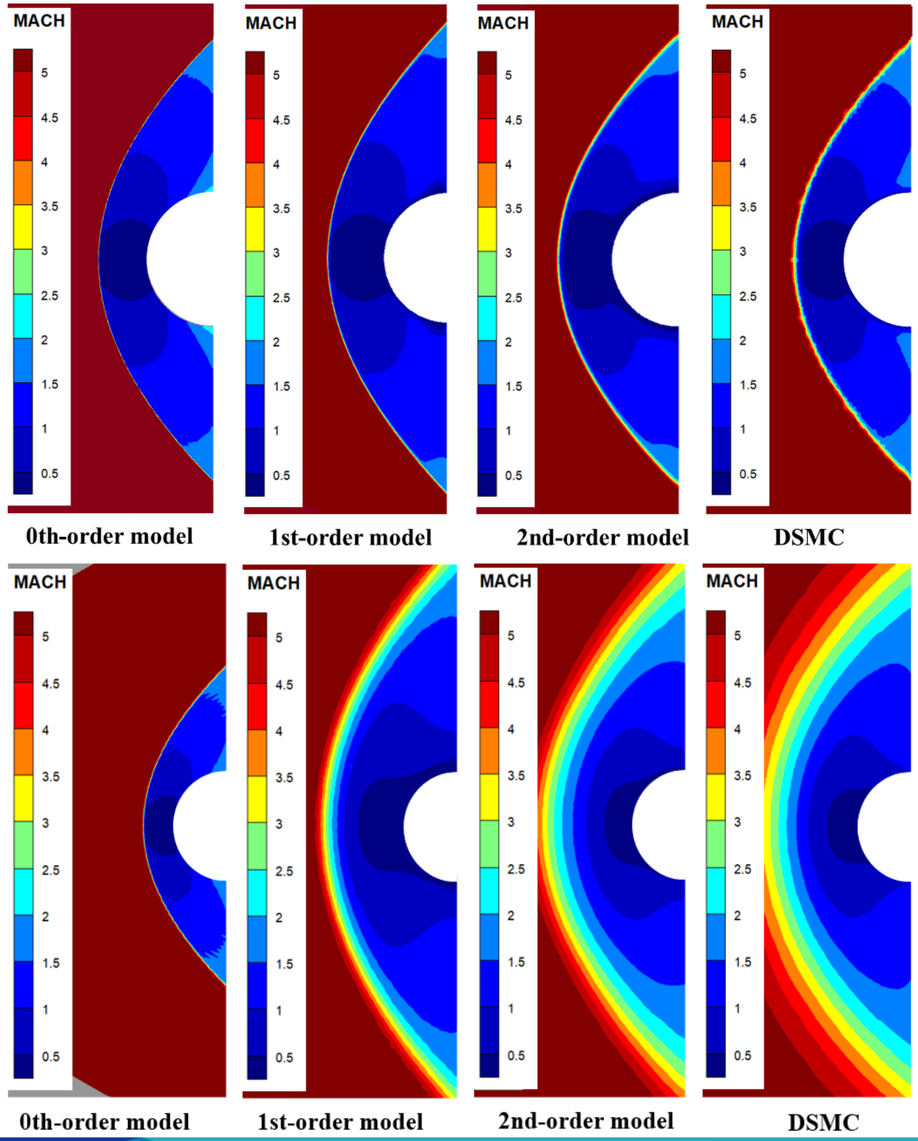

Argon gas

Mach 5.48

Knudsen 0.02

Argon gas

Mach 5.48

Knudsen 0.2

A body with side-jet: DACS (Divert Attitude Control System)

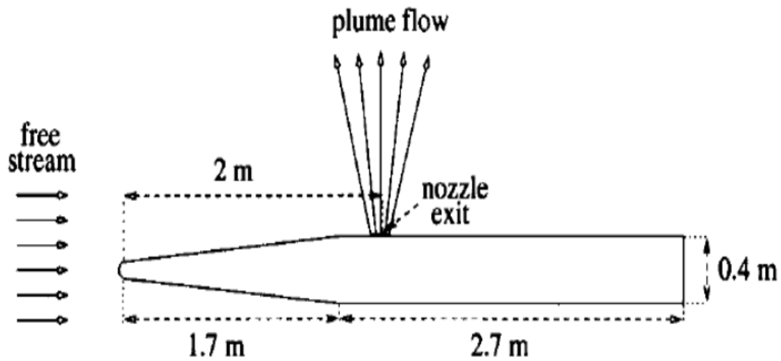

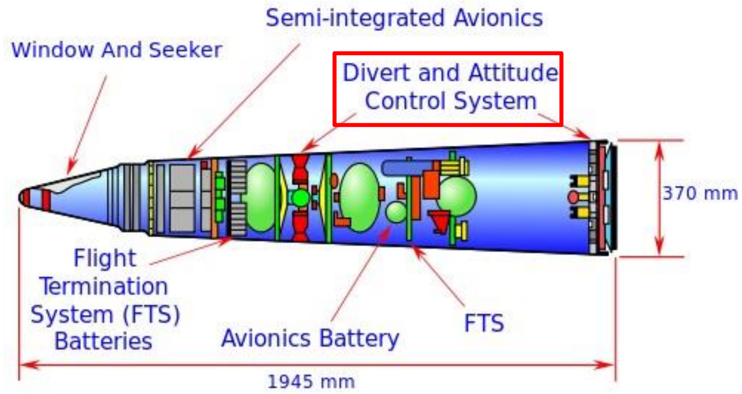

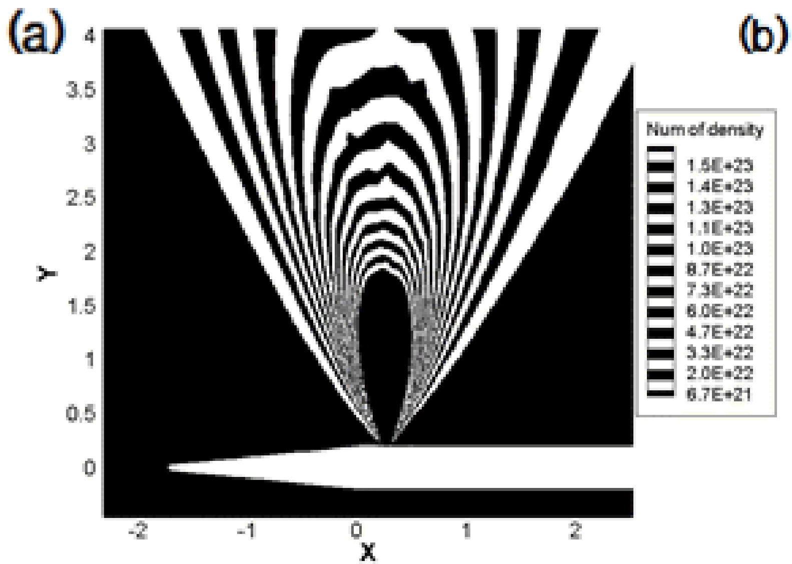

NCCR-DG

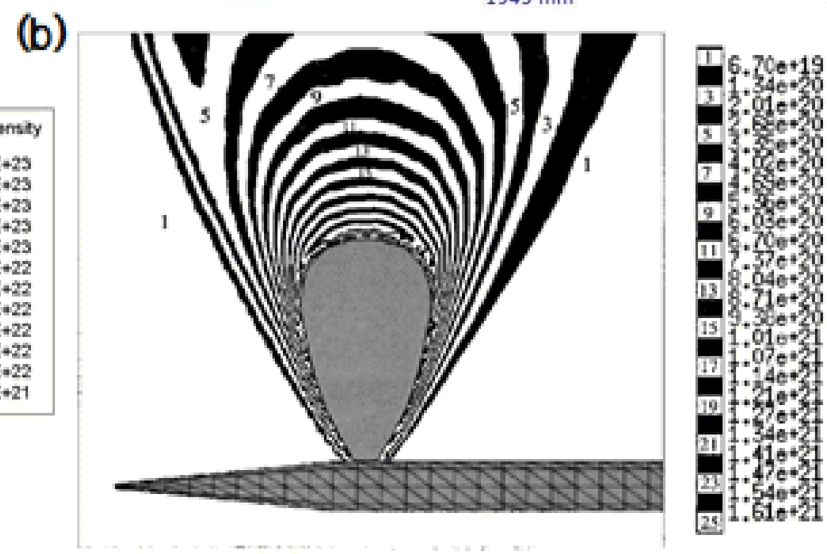

DSMC

Number of density contour (nitrogen gas, velocity=2km/s, Knudsen=0.1)

Full 3-D hypersonic rarefied flows around a vehicle

A suborbital re-entry vehicle

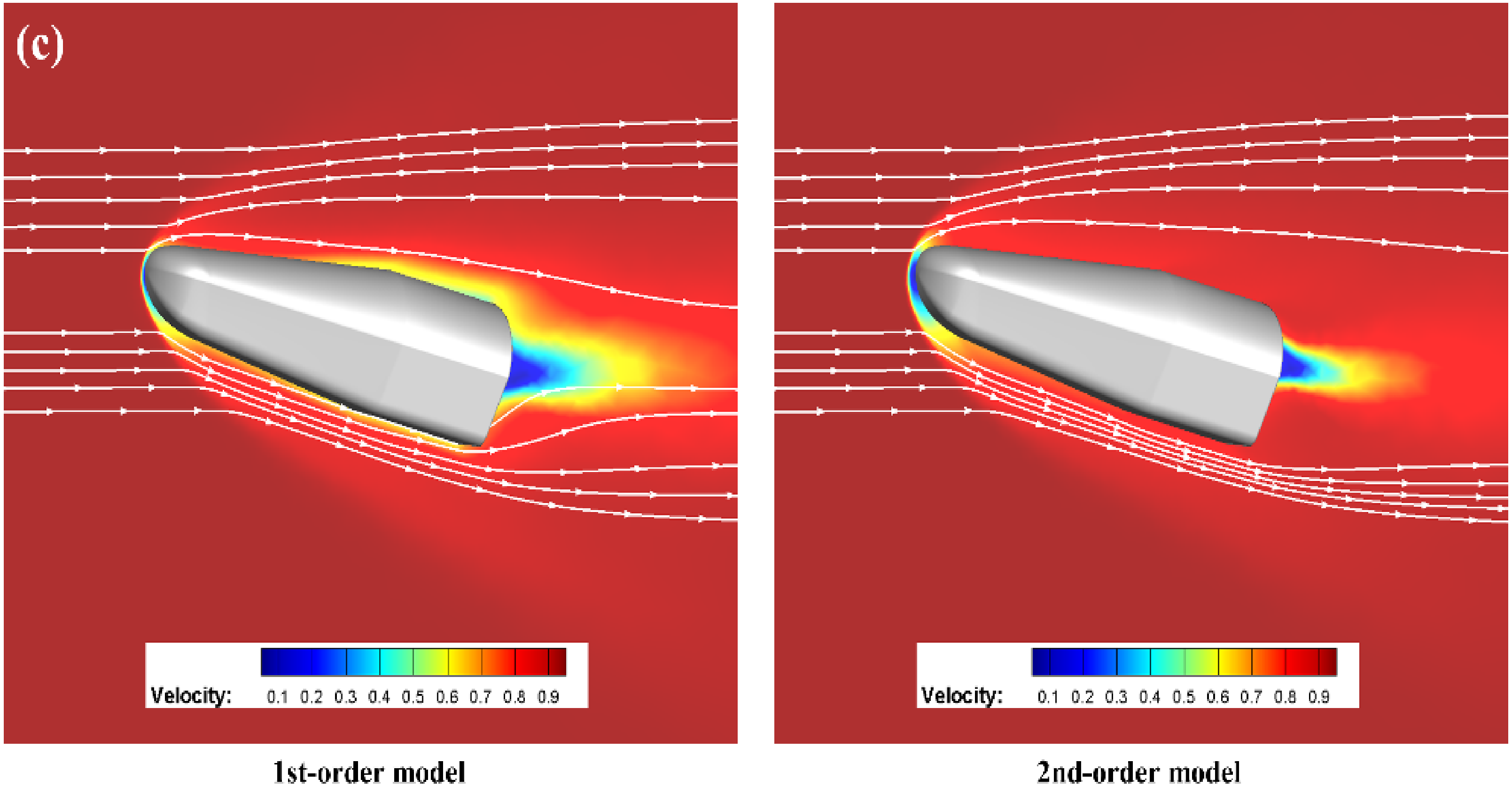

Velocity contours of nitrogen gas flows; Mach 5.0, Knudsen 0.02

Future topics: scientific aspect

Non-classical flow physics including mixture, chemical reaction and radiation modeling

Extension to multi-phase flow problems

Aerothermodynamic data for design and control

More accessible (via OpenFOAM of NCCR-FVM) and efficient computational algorithms

Combination with machine learning and quantum computing

Related journal papers

- Myong, R. S., Thermodynamically Consistent Hydrodynamic Computational Models for High-Knudsen-Number Gas Flows, ***Physics of Fluids***, Vol. 11, No. 9, pp. 2788-2802, **1999**.
- Myong, R. S., On the High Mach Number Shock Structure Singularity Caused by Overreach of Maxwellian Molecules, ***Physics of Fluids***, Vol. 26, No. 5, 056102, **2014**.
- Mankodi, T. K., Myong, R. S., Quasi-classical Trajectory-based Non-equilibrium Chemical Reaction Models for Hypersonic Air Flows, ***Physics of Fluids***, Vol. 31, 106102, **2019.**
- Singh, S., Karchani, A., Sharma, K., Myong, R. S., Topology of the Second-Order Constitutive Model Based on the Bolzmann-Curtiss Kinetic Equation for Diatomic and Polyatomic Gases, ***Physics of Fluids***, Vol. 32, 026104, **2020**.
- Mankodi, T. K., Myong, R. S., Boltzmann-based Second-order Constitutive Models of Diatomic and Polyatomic Gases including the Vibrational Mode, **Physics of Fluids**, Vol. 32, 126109, **2020**.
- Chae, J. H., Mankodi, T. K., Choi, S. M., Myong, R. S., Combined Effects of Thermal Non-equilibrium and Chemical Reactions on Hypersonic Air Flows Around An Orbital Reentry Vehicle, ***International Journal of Aeronautical and Space Science***, Vol. 21, pp. 612-626, **2020**.
- Singh, S., Karchani, A., Chourushi, T., Myong, R. S., A Three-Dimensional Modal Discontinuous Galerkin Method for the Second-Order Boltzmann-Curtiss-Based Constitutive Model of Rarefied and Microscale Gas Flows, ***Journal of Computational Physics***, Vol. 457, 111052, **2022**.